Date of publication xxxx 00, 0000, date of current version xxxx 00, 0000.

Digital Object Identifier 10.1109/ACCESS.2017.DOI

Artificial-Noise-Aided Precoding Design for Multi-User Visible Light Communication Channels

THANH V. PHAM[1], (Student Member, IEEE), TAKAFUMI HAYASHI[2], (Member, IEEE), and ANH T. PHAM[1], (Senior Member, IEEE)

[1]Computer Communications Laboratory, The University of Aizu, Aizuwakamatsu, Fukushima 965-8580, Japan.
[2]Department of Information Engineering, Niigata University, Niigata 950-2181, Japan.

Corresponding author: Thanh V. Pham (e-mail: lete143@gmail.com).

This work was supported in part by JSPS KAKENHI 18J14290 and 15K00134.

ABSTRACT This paper studies the physical layer security in visible light communications (VLC) networks with multiple users when there is a single wiretap eavesdropper. In particular, we investigate different designs of artificial noise (AN)-aided precoding scheme to improve the secrecy performance in terms of legitimate users and eavesdropper's signal-to-interference-plus-noise ratios (SINRs). To guarantee fair performance among users, the purpose of the AN-aid precoding designs is to solve the max-min fairness SINR problem among legitimate users for two different scenarios: unknown and known eavesdropper's channel state information (CSI) at the transmitters. In the former case, we adopt the traditional null-space AN scheme and then study the impact of the AN power on the fairness performance. In the case of known eavesdropper's CSI, the AN-aided precoding is designed in such a way that it keeps the SINR of the eavesdropper below a predefined threshold. Furthermore, we also study specific cases of AN-aided design with the zero-forcing (ZF) technique and compare its performance with the general one. In both designs, numerical results show that significant gaps between users' and eavesdropper's SINR can always be achieved, thus guaranteeing a high secrecy performance. It is also observed that while the general design outperforms the ZF one in terms of users' SINRs, it does not degrade the eavesdropper's channel quality as much as the ZF design does, especially in the low transmit power region.

INDEX TERMS multi-user VLC, physical layer security, artificial noise, linear precoding.

I. INTRODUCTION

Recent advances in solid-state lighting has enabled high speed visible light communications (VLC), which is regarded as a promising complement to the existing wireless technologies. The immunity of visible light signal to other electromagnetic sources makes VLC suitable for indoor applications. Due to the widespread utilization of light-emitting diodes (LEDs), it is conceivable that VLC will also play an important role in the future ubiquitous networking [1], [2].

In order to provide a sufficient and uniform illumination over a target plane, indoor lighting systems usually require deployment of multiple LED arrays (LED fixtures). Since each LED array can act as a transmitting device, this configuration inherently creates the multiple-input multiple-output (MIMO) transmission scheme, which, by means of spatial multiplexing, considerably improves the data rate for VLC systems [3]–[7]. On one hand, due to the broadcast nature of visible light, VLC can be categorized as broadcast systems, which are capable of serving multiple users. As a result, there has been an increasing interest in studying multi-user MIMO-VLC broadcast systems over the past few years [8]–[10]. On the other hand, the broadcast nature of visible light signal presents a challenge in guaranteeing secure communications in the presence of unauthorized users. That is, any users within the illuminated area can gain accessibility of the transmitted signal, thus making eavesdropping a possible threat. Traditionally, the security of data transmission is performed at network and transport layers by means of key-based cryptographic techniques. In addition to security at upper layers, security at the physical layer (also known as physical layer security) has been emerging as a new approach to deal with eavesdropping. In his foundational work on physical layer

security, A. D. Wyner introduced the concept of wiretap channel, which consists of a transmitter, a legitimate user and an eavesdropper [11]. Then, the main concern was on characterizing the *secrecy capacity*, which is defined as the maximum reliable information rate at which the transmitted message cannot be decoded by eavesdroppers regardless of their computational power and knowledge of the encoding scheme [12], [13].

In the context of VLC, its inherent MIMO configuration introduces a spatial degrees of freedom, which can be utilized in the forms of precoding (i.e., beamforming) and/or artificial noise (AN) to enhance the secrecy capacity. In particular, precoding techniques were thoroughly investigated for single [14]–[16] and multi-user configurations [17] under both perfect and uncertain channel state information (CSI) of the eavesdropper. The authors in [18] studied the secrecy outage probability (SOP) for a system consisting of multiple random distributed eavesdroppers. Based on the same performance metric (i.e., SOP), the work in [19] investigated the use of non-orthogonal multiple access (NOMA) in multi-user multi-eavesdropper VLC systems. Most recently, a comprehensive analysis on the secrecy capacity of the traditional VLC wiretap channel (i.e., one transmitter, one legitimate user and one eavesdropper) has been reported in [20]. As for the AN approach, to the best of our knowledge, all previous studies focused on the single legitimate user configuration only. Specifically, in [21] and [22], the AN was generated by a set of LED transmitters to jam the eavesdropper's channel. The rest of the LED transmitters were then used for transmitting the information-bearing signal to the legitimate user. On the other hand, the AN could also be added to the precoded information-bearing signal as studied in recent works [23], [24]. The combined signal was then transmitted by all LED transmitters. This approach (known as AN-aided precoding) involves precoding designs for the AN and the information-bearing signals.

Due to the lack of the AN design approach for physical layer security in multi-user VLC wiretap channels, we attempt to fill this gap in this paper. It is known that the modulating signal in VLC is subject to amplitude constraint, which makes characterizing the channel capacity a challenging task [26]. In fact, closed-form expressions for the capacity of an amplitude constrained channel are not available. The AN-aided precoding design with respect to the secrecy capacity would be cumbersome, especially in the case of multiple users. In this paper, we therefore investigate an alternative approach for the AN-aided precoding design in multi-user VLC wiretap channels by considering the QoS-based perspective. In the conference version of the paper [25], we studed the problem of max-min fairness signal-to-interference-plus-noise ratio (SINR) among multiple legitimate users under the presence of an eavesdropper whose CSI can be either known or unknown to the transmitters. In the case of unknown eavesdropper's CSI, the AN was designed to lie in the null space of users' channel matrices. We then investigated the impact of the AN noise power on the performances of users and the eavesdropper. In case the eavesdropper's CSI is available, the AN-aided precoding was designed taking into account a constraint that the eavesdropper's SINR is kept below a predefined threshold. In addition to the general design, in this paper, a specific design, which adopts the zero-forcing (ZF) technique as the underlaying precoding scheme for legitimate users, is also investigated. A comprehensive comparison between the performances of general and ZF designs is then given.

The rest of the paper is structured as follows. In Section II, a multi-user VLC wiretap channel together with AN-aided precoding models are described. Section III investigates the general AN-aided precoding designs for two cases of known and unknown eavesdropper's CSI. A specific design using ZF precoding scheme is presented in Section IV. Representative numerical results are presented in Section V. Finally, we conclude the paper in Section VI.

Notation: The following notations are used throughout the paper. $\mathbb{R}$ and $\mathbb{E}[\cdot]$ are the set of real-valued numbers and the expected value operator, respectively. Bold upper case letters denotes matrices, e.g., $\mathbf{A}$ while the transpose of $\mathbf{A}$ is written as $\mathbf{A}^T$. $\|\cdot\|_1$ and $\|\cdot\|_F$ are the L_1 norm and the Frobenius norm, respectively. $\mathbf{I}_N$ denotes the identity matrix of size N, $\mathbf{e}_n$ is the all zero vector with the $n-$th element being 1, $\mathbf{1}_N$ is the all one vector of size N, $\mathbf{0}_{M\times N}$ is all zero matrix of size $M \times N$. Finally, $\mathbf{A} \otimes \mathbf{B}$ and $\mathbf{A} \circ \mathbf{B}$ represent the Kronecker and the Hadamard products of matrices $\mathbf{A}$ and $\mathbf{B}$.

II. MULTI-USER WIRETAP VLC CHANNEL MODEL

A. VLC CHANNEL MODEL

As illustrated in Fig. 1, we consider in this paper a multi-user VLC broadcast network, which consists of N_T LED arrays acting as the transmitters, K non-cooperative legitimate users and an eavesdropper. Assume that users and the eavesdropper are equipped with a photodiode (PD). In practice, most LED sources have Lambertian beam distribution where the emission intensity is given by

$$L(\phi) = \frac{l+1}{2\pi}\cos^l(\phi), \tag{1}$$

where ϕ is the angle of irradiance and l is the order of Lambertian emission determined by the semi-angle for half illuminance of the LED $\Phi_{1/2}$ as $l = -\frac{\log(2)}{\log(\Phi_{1/2})}$ [27]. If we denote $h_{n,k}$ as the light-of-sight (LOS) channel response coefficient between the $n-$th LED array and the $k-$th legitimate user, it is given by

$$h_{n,k} = \begin{cases} \frac{A_r}{t_{n,k}^2} L(\phi) T_s(\psi_{n,k}) g(\psi_{n,k}) \cos(\psi_{n,k}) & , 0 \le \psi_{n,k} \le \Psi, \\ 0 & , \psi_{n,k} > \Psi, \end{cases} \tag{2}$$

where A_r and $t_{n,k}$ are the active area of the PD and the distance from the LED array to the user, respectively [27]. Ψ denotes the optical field of view (FOV) of the PD, $\psi_{n,k}$ is the angle of incidence and $T_s(\psi_{n,k})$ is the gain of the optical

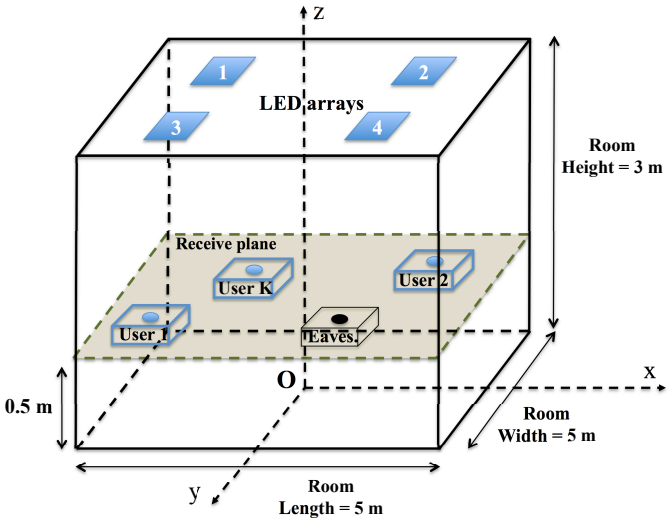

Figure 1: A geometrical configuration of a multi-user VLC network with an eavesdropper.

filter, whereas $g(\psi_{n,k})$ is the gain of the optical concentrator and given by

$$g(\psi_{n,k}) = \begin{cases} \frac{\kappa^2}{\sin^2 \Psi} & , 0 \leq \psi_{n,k} \leq \Psi, \\ 0 & , \psi_{n,k} > \Psi, \end{cases} \tag{3}$$

where κ is the refractive index of the concentrator.

B. AN-AIDED PRECODING MODEL

Let $d_k \in \mathbb{R}$ be the data symbol drawn from pulse amplitude modulation (PAM) that is intended to the $k-$th user and $\mathbf{d} = \begin{bmatrix} d_1 & d_2 & \dots & d_K \end{bmatrix}^T \in \mathbb{R}^{K\times 1}$ be the data vector of legitimate users. Without loss of generality, suppose that d_k is zero mean and is normalized to the range of $[-1, 1]$. At the $n-$th LED array transmiter, the information-bearing signal s_n is generated from a linear combination of the data vector and a precoding matrix $\mathbf{V}_n = \begin{bmatrix} w_{n,1} & w_{n,2} & \dots & w_{n,K} \end{bmatrix} \in \mathbb{R}^{1\times K}$ as

$$s_n = \mathbf{V}_n \mathbf{d}. \tag{4}$$

In what follows, the AN-aided precoding models are explicitly described for two scenarios: unknown and known eavesdropper's CSI at the transmitters.

1) Unknown Eavesdropper's CSI

When the eavesdropper's CSI is not available at the transmitters, the AN should be designed in such a way that it is orthogonal to the information-bearing signal. By doing so, the AN would not interfere the legitimate users but potentially degrades the eavesdropper's channel. Let $\mathbf{H}_k = \begin{bmatrix} h_{1,k} & h_{2,k} & \dots & h_{N_T,k} \end{bmatrix} \in \mathbb{R}^{1\times N_T}$ be the channel matrix of the $k-$th user, and $\mathbf{H} = \begin{bmatrix} \mathbf{H}_1^T & \mathbf{H}_2^T & \dots & \mathbf{H}_K^T \end{bmatrix}^T \in \mathbb{R}^{K\times N_T}$ be the aggregate matrix of all legitimate users. Assume that $\mathbf{H}$ is full row-rank and let $\mathbf{G}$ is an orthonormal basis for the null-space of $\mathbf{H}$. According the rank-nullity theorem, $\text{rank}(\mathbf{H}) + \dim(\mathbf{G}) = N_T$. Since $\text{rank}(\mathbf{H}) = K$, $\mathbf{G}$ has a dimension of $(N_T - K)$. It can obviously seen that this AN design is not feasible when $N_T \leq K$. Throughout this paper, we thus assume that $N_T > K$. Denote $\mathbf{z} = \begin{bmatrix} z_1 & z_2 & \dots & z_{N_T-K} \end{bmatrix}^T \in \mathbb{R}^{(N_T-K)\times 1}$ as the AN noise vector, which is added into the information-bearing signal s_n. It is also assumed that each element z_i is zero mean and is normalized to $[-1, 1]$. The broadcast signal at the $n-$th LED array can be written as

$$x_n = s_n + \rho_n \mathbf{G}_n \mathbf{z}, \tag{5}$$

where $\mathbf{G}_n \in \mathbb{R}^{1\times(N_T-K)}$ is the $n-$th row vector of the orthonormal basic $\mathbf{G}$ and ρ_n is a constant, which controls the amplitude of the AN signal at the $n-$th LED transmitter. It is seen that x_n can take on negative values, which are not valid for the intensity modulation/direct detection (IM/DD) used in VLC systems. Thus, a DC-bias should be added into x_n to ensure that it is non-negative, i.e.,

$$u_n = x_n + I_n^{\text{DC}} \geq 0, \tag{6}$$

where I_n^{DC} is the DC-bias for the $n-$th LED array. As $\mathbb{E}[\mathbf{d}] = 0$ and $\mathbb{E}[\mathbf{z}] = 0$, the signal x_n does not affect the average illumination level of the LED arrays. Instead, it is uniquely determined by the DC-bias I_n^{DC}. If we define $\mathbf{P}^s = \begin{bmatrix} P_1^s & P_2^s & \dots & P_{N_T}^s \end{bmatrix}^T$ as the transmitted optical vector of the LED arrays whose element $P_n^s = \eta u_n$ is the transmitted power of the $n-$th LED array with η being the LED conversion factor, the received optical signal at the $k-$th user can be written as

$$P_k^s = \mathbf{H}_k \mathbf{P}_k^s. \tag{7}$$

Let us define $\mathbf{u} = \begin{bmatrix} u_1 & u_2 & \dots & u_{N_T} \end{bmatrix}^T$ and $\mathbf{I}^{\text{DC}} = \begin{bmatrix} I_1^{\text{DC}} & I_2^{\text{DC}} & \dots & I_{N_T}^{\text{DC}} \end{bmatrix}^T$ as the transmitted signal vector and the DC-bias vector, respectively. The received electrical signal is then given by

$$\begin{aligned} y_k &= \gamma P_k^r + n_k = \gamma\eta \mathbf{H}_k \mathbf{u} + n_k \\ &= \gamma\eta \left(\mathbf{H}_k \mathbf{W}_k d_k + \mathbf{H}_k \sum_{i=1, i\neq k}^{K} \mathbf{W}_i d_i + \mathbf{H}_k \mathbf{I}^{\text{DC}} \right) \\ &\quad + n_k, \end{aligned} \tag{8}$$

with $\mathbf{W}_k = \begin{bmatrix} w_{1,k} & w_{2,k} & \dots & w_{N_T,k} \end{bmatrix}^T$ being the precoding matrix for the $k-$th user, γ being the PD responsivity. The receiver noise n_k is assumed to be additive white Gaussian noise (AWGN) with zero mean and variance σ_k^2 given by [3]

$$\sigma_k^2 = 2\gamma e \overline{P_k^r} B + 4\pi e A_r \gamma \chi_{\text{amb}} (1 - \cos(\Psi)) B + i_{\text{amp}}^2 B, \tag{9}$$

where e is the elementary charge, B denotes the system bandwidth and $\overline{P_k^r} = \mathbb{E}[P_k^r] = \eta \mathbf{H}_k \mathbf{I}^{\text{DC}}$ is the average received optical power at the $k-$th user. i_{amp}^2 is the pre-amplifier noise current density, χ_{amb} is the ambient light

photocurrent. After removing the DC current term $\mathbf{H}_k\mathbf{I}^{\mathrm{DC}}$ by AC coupling, the received signal can be written by

$$y_k = \gamma\eta\left(\mathbf{H}_k\mathbf{W}_k d_k + \mathbf{H}_k\sum_{i=1,i\neq k}^{K}\mathbf{W}_i d_i\right) + n_k. \quad (10)$$

Similarly, the received electrical signal at the eavesdropper is given by

$$y_e = \gamma\eta\left(\mathbf{H}_e\sum_{i=1}^{K}\mathbf{W}_i d_i + \mathbf{H}_e\left(\boldsymbol{\rho}\circ\mathbf{G}\right)\mathbf{z}\right) + n_e, \quad (11)$$

where $\mathbf{H}_e$ is the channel matrix of the eavesdropper and $\boldsymbol{\rho} = \begin{bmatrix}\rho_1 & \rho_2 & \dots & \rho_{N_T}\end{bmatrix}^T$.

2) Known Eavesdropper's CSI

In case the eavesdropper's CSI is available at the transmitters, the AN is not necessary to be orthogonal to the information-bearing signal. By knowing eavesdropper's CSI, the transmitters optimally design the AN to meet the requirements on users' SINRs while keeping the SINR of the eavesdropper below a pre-described threshold. In this case, let us denote $\widetilde{\mathbf{z}} = \begin{bmatrix}\widetilde{z}_1 & \widetilde{z}_2 & \dots & \widetilde{z}_{N_T}\end{bmatrix}^T \in \mathbb{R}^{N_T\times 1}$ as the AN noise vector and $\widetilde{\mathbf{G}} \in \mathbb{R}^{N_T\times N_T}$ as its precoder, which can be an arbitrary matrix. Similar to the case of unknown eavesdropper's CSI, each element $\widetilde{z}_i$ of $\widetilde{\mathbf{z}}$ is assumed to be zero mean and normalized to $[-1, 1]$. The received signals at the $k-$th user and at the eavesdropper are then expressed by

$$y_k = \gamma\eta\left(\mathbf{H}_k\mathbf{W}_k d_k + \mathbf{H}_k\sum_{i=1,i\neq k}^{K}\mathbf{W}_i d_i + \mathbf{H}_k\widetilde{\mathbf{G}}\widetilde{\mathbf{z}}\right) + n_k, \quad (12)$$

and

$$y_e = \gamma\eta\left(\mathbf{H}_e\sum_{i=1}^{K}\mathbf{W}_i d_i + \mathbf{H}_e\widetilde{\mathbf{G}}\widetilde{\mathbf{z}}\right) + n_e, \quad (13)$$

respectively.

C. OPTICAL POWER CONSTRAINT

Following the arguments described [10], to guarantee normal operations of the LEDs and ensure energy efficiency, the drive current u_n must be constrained within the range $[0, I_{\max}]$, where the output optical power increases linearly with an increase in the drive current as illustrated in Fig. 2. The constraint is reflected in the following inequalities

$$0 \leq x_n + I_n^{\mathrm{DC}} \leq I_{\max}. \quad (14)$$

For the case of unknown eavesdropper's CSI, since $|d_i| \leq 1$ and $|z_i| \leq 1$, we get

$$-\left(\|\mathbf{V}_n\|_1 + \rho_n\|\mathbf{G}_n\|_1\right) \leq x_n \leq \left(\|\mathbf{V}_n\|_1 + \rho_n\|\mathbf{G}_n\|_1\right). \quad (15)$$

With respect to the precoding matrix $\mathbf{W}_k$ and to ensure both (14) and (15), the following constraint should be imposed

$$\sum_{i=1}^{K}\|[\mathbf{W}_k]_n\|_1 + \rho_n\|\mathbf{G}_n\|_1 \leq \Delta_n, \quad (16)$$

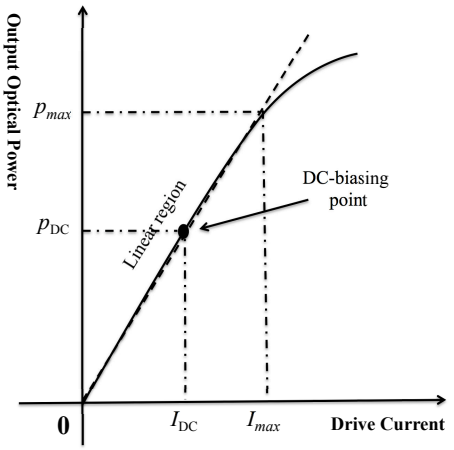

Figure 2: Nonlinear LED transfer characteristic.

with $\Delta_n = \min\left(I_n^{\mathrm{DC}}, I_{\max} - I_n^{\mathrm{DC}}\right)$ and $[\mathbf{W}_k]_n$ being the n-th row vector of $\mathbf{W}_k$.

Similarly, in the case of known eavesdropper's CSI, we have the following constraint on precoders design

$$\sum_{i=1}^{K}\|[\mathbf{W}_k]_n\|_1 + \|\widetilde{\mathbf{G}}_n\|_1 \leq \Delta_n, \quad (17)$$

where $\widetilde{\mathbf{G}}_n$ is the $n-$th row vector of $\widetilde{\mathbf{G}}$.

III. GENERAL AN-AIDED PRECODING DESIGNS

A. UNKNOWN EAVESDROPPER'S CSI

It is known that the uniform distribution is the maximum entropy probability distribution for a random variable under no constraint other than it is contained in the distribution's support [28]. Hence, to maximize users' SINRs as well as the interference caused by the AN at the eavesdropper, let us assume that d_k and z_k are both uniformly distributed over $[-1, 1]$. From (10) and (11), the SINR of the $k-$th legitimate user and the eavesdropper are then given by

$$\mathrm{SINR}_k = \frac{\theta^2\left|\mathbf{H}_k\mathbf{W}_k\right|^2}{\theta^2\sum\limits_{i=1,i\neq k}^{K}\left|\mathbf{H}_k\mathbf{W}_i\right|^2 + \sigma_k^2}, \quad (18)$$

and

$$\mathrm{SINR}_{e,k} = \frac{\theta^2\left|\mathbf{H}_e\mathbf{W}_k\right|^2}{\theta^2\sum\limits_{i=1,i\neq k}^{K}\left|\mathbf{H}_e\mathbf{W}_i\right|^2 + \theta^2\left\|\mathbf{H}_e\left(\boldsymbol{\rho}\circ\mathbf{G}\right)\right\|_F^2 + \sigma_e^2}, \quad (19)$$

respectively, where $\theta = \frac{1}{\sqrt{3}}\gamma\eta$. Note that $\mathrm{SINR}_{e,k}$ is the SINR of the eavesdropper corresponding to the data symbol d_k it eavesdrops on the $k-$th user. In the considered system with K users, there are thus K values of the eavesdropper's SINRs for users' data symbols. Since $\mathbf{H}_e$ is unknown to the transmitters, the precoding matrices $\mathbf{W}_k$ are designed to solve the legitimate user SINR max-min fairness problem

regardless of the eavesdropper's SINR. The problem is formulated as follows

$$\mathcal{P}1: \underset{\mathbf{W}_k}{\text{maximize}} \quad \min_k \ \text{SINR}_k \quad \text{subject to} \quad \sum_{i=1}^{K} \|[\mathbf{W}_k]_n\|_1 + \rho_n \|\mathbf{G}_n\|_1 \le \Delta_n. \tag{20}$$

To ensure the feasibility of $\mathcal{P}1$, ρ_n's should be chosen to satisfy the inequality constraints. In principle, ρ_n's are set individually depending on the AN power allocated in each LED transmitter. In fact, setting ρ_n's individually can further improve the secrecy performance. For example, maximum AN power should be allocated to transmitters, which do not associate with any users. By doing so, the chance of degrading the eavesdropper's channel by AN can be considerably higher. However, for the sake of simplicity, we assume that ρ_n's are equal (i.e., $\rho_i = \rho_j = \rho$). Then, one can set $\rho = \frac{\overline{p} \min \Delta_n}{\max \|\mathbf{G}_n\|_1}$, where $\overline{p}$ $(0 \le \overline{p} \le 1)$ is a constant which controls the amplitude of the AN in the sense that the larger the $\overline{p}$ is, the higher the AN amplitude (i.e., power) becomes. By introducing a slack variable t, $\mathcal{P}1$ can be rewritten as

$$\mathcal{P}2: \underset{\mathbf{W}_k, t}{\text{maximize}} \quad t \quad \text{subject to} \quad \frac{|\mathbf{H}_k \mathbf{W}_k|^2}{\sum_{i=1, i\neq k}^{K} |\mathbf{H}_k \mathbf{W}_i|^2 + \sigma_k'^2} \ge t, \quad \sum_{i=1}^{K} \|[\mathbf{W}_k]_n\|_1 \le \Delta_{\overline{p},n}, \tag{21}$$

where $\sigma_k'^2 = \sigma_k^2/\theta^2$ and $\Delta_{\overline{p},n} = \Delta_n - \frac{\overline{p} \min \Delta_n}{\max \|\mathbf{G}_n\|_1} \|\mathbf{G}_n\|_1$. It can be seen that the first constraint of $\mathcal{P}2$ is not convex, thus the problem is difficult to solve. A standard approach to handle the problem is to reformulate it to a convex optimization for a fixed t and then using the bisection method to solve the reformulated problem. Following the same procedure in [29], let $\mathbf{W} = \begin{bmatrix} \mathbf{W}_1 & \mathbf{W}_2 & \dots & \mathbf{W}_K \end{bmatrix} \in \mathbb{R}^{N_T \times K}$, $w = \text{vec}(\mathbf{W}^T)$, and $\mathbf{I}_K^k$ be the matrix obtained from the identity matrix of size K by setting the $(k,k)-$th element be zero. Now, for a fixed value of t, we solve the following feasibility problem

$$\mathcal{P}3: \text{find} \quad \mathbf{w} \quad \text{subject to} \quad \|\mathbf{B}_k \mathbf{w} + \boldsymbol{\sigma}'_k\|_F \le \frac{1}{\sqrt{t}} \mathbf{H}_k (\mathbf{I}_{N_T} \otimes \mathbf{e}_k^T) \mathbf{w}, \quad -\mathbf{a} \le \mathbf{w} \le \mathbf{a}, \quad \mathbf{U}\mathbf{a} \le \boldsymbol{\Delta}_{\overline{\rho}}, \tag{22}$$

where $\mathbf{B}_k = \begin{bmatrix} \mathbf{H}_k \otimes \mathbf{I}_K^k \\ \mathbf{0}_{1 \times N_T K} \end{bmatrix}$, $\boldsymbol{\sigma}'_k = \begin{bmatrix} \mathbf{0}_{1\times K} & \sigma'_k \end{bmatrix}^T$, $\mathbf{U} = \mathbf{I}_{N_T} \otimes \mathbf{1}_K^T$, $\boldsymbol{\Delta}_{\overline{\rho}} = \begin{bmatrix} \Delta_{\overline{\rho},1} & \Delta_{\overline{\rho},2} & \dots & \Delta_{\overline{\rho},N_T} \end{bmatrix}^T$, and $\mathbf{a} = \begin{bmatrix} a_1 & a_2 & \dots & a_{N_T K} \end{bmatrix}^T$ is a new optimization variable. The above problem is a second-order cone program (SOCP) [32], which is convex and can be solved efficiently using off-the-self optimization packages [34], [35]. The optimal t is the maximum value for which $\mathbf{w}$ exists and satisfies the constraints in $\mathcal{P}3$. Therefore, the optimal value of t can be found by bisection algorithm as described in detail in [29]. The algorithm is presented here for the sake of convenience.

Algorithm 1 Bisection algorithm for solving problem $\mathcal{P}3$

1) Estimate channel matrices $\mathbf{H}_k$, $\mathbf{H}_e$ and noise variances σ_k^2, σ_e^2.
2) Initialize t_1 and t_2 $(t_1 < t_2)$ so that $\mathcal{P}3$ is infeasible when $t = t_2$ and feasible when $t = t_1$.
3) Initialize a tolerance parameter ϵ.

while $t_2 - t_1 > \epsilon$ **do**
  $t = (t_1 + t_2)/2$.
  Solve the feasibility of $\mathcal{P}3$ by CVX toolbox.
  if the problem is feasible **then** $t_1 = t$.
  else $t_2 = t$.
  end if
end while

The optimal precoder $\mathbf{W}_k^*$ is given by $\mathbf{W}_k^* = (\mathbf{I}_{N_T} \otimes \mathbf{e}_k^T)\widetilde{\mathbf{w}}$, where $\widetilde{\mathbf{w}}$ is the last feasible solution to $\mathcal{P}3$ (i.e., the solution to $\mathcal{P}3$ for $t = t_1$).

B. KNOWN EAVESDROPPER'S CSI

In this case, the SINRs of the $k-$th legitimate user and the eavesdropper are given by

$$\text{SINR}_k = \frac{|\mathbf{H}_k \mathbf{W}_k|^2}{\sum_{i=1, i\neq k}^{K} |\mathbf{H}_k \mathbf{W}_i|^2 + \left\|\mathbf{H}_k \widetilde{\mathbf{G}}\right\|_F^2 + \sigma_k'^2}, \tag{24}$$

and

$$\text{SINR}_{e,k} = \frac{|\mathbf{H}_e \mathbf{W}_k|^2}{\sum_{i=1, i\neq k}^{K} |\mathbf{H}_e \mathbf{W}_i|^2 + \left\|\mathbf{H}_e \widetilde{\mathbf{G}}\right\|_F^2 + \sigma_e'^2}, \tag{25}$$

respectively, where $\sigma_e'^2 = \sigma_e^2/\theta^2$. Different from the previous case, since the eavesdropper's CSI is available at the transmitter, the eavesdropper's SINR can be controlled by the AN. Taking into account the eavesdropper's SINR in the precoder designs, the max-min fairness problem is then formulated as follows

$$\mathcal{P}4: \underset{\mathbf{W}_k, \widetilde{\mathbf{G}}}{\text{maximize}} \quad \min_k \ \text{SINR}_k \quad \text{subject to} \quad \text{SINR}_{e,k} \le \lambda_k, \quad \sum_{i=1}^{K} \|[\mathbf{W}_k]_n\|_1 + \left\|\widetilde{\mathbf{G}}_n\right\|_1 \le \Delta_n, \tag{26}$$

where λ_k is the maximum allowable SINR threshold imposed on the eavesdropper for the eavesdropped data symbol d_k. Obviously, problem $\mathcal{P}4$ is more complex than $\mathcal{P}1$ due to additional non-convex constraints on the eavesdropper's SINRs and the optimization is over both precoding matrices $\mathbf{W}_k$ and $\widetilde{\mathbf{G}}$. However, the same procedure can be applied to solve the

$$
\begin{aligned}
\mathcal{P}7: \ \text{find} \quad & \mathbf{q}^{(i)} \\
\text{subject to} \quad & \left\|\mathbf{B}_k\mathbf{q}^{(i)}+\boldsymbol{\sigma'}_k\right\|_F \le \frac{1}{\sqrt{t}}\mathbf{H}_k\left(\mathbf{I}_{N_T}\otimes(\mathbf{e}_k^T\mathbf{V})\right)\mathbf{q}^{(i)}, \\
& \left\|\mathbf{B}_{e,k}\mathbf{q}^{(i-1)}+\boldsymbol{\sigma'}_e\right\|_F + \frac{\left[\mathbf{B}_{e,k}\mathbf{q}^{(i-1)}+\boldsymbol{\sigma'}_e\right]^T\mathbf{B}_{e,k}}{\left\|\mathbf{B}_{e,k}\mathbf{q}^{(i-1)}+\boldsymbol{\sigma'}_e\right\|_F}\left(\mathbf{q}^{(i)}-\mathbf{q}^{(i-1)}\right) \ge \frac{1}{\sqrt{\lambda_k}}\mathbf{H}_e\left(\mathbf{I}_{N_T}\otimes(\mathbf{e}_k^T\mathbf{V})\right)\mathbf{q}^{(i)}, \\
& -\mathbf{a}\le\mathbf{q}^{(i)}\le\mathbf{a}, \\
& \mathbf{U}\mathbf{a}\le\boldsymbol{\Delta}.
\end{aligned} \tag{23}
$$

problem. Similar to the previous case, we transform it to the following equivalent form

$$
\begin{aligned}
\mathcal{P}5: \ \underset{\mathbf{W}_k,\widetilde{\mathbf{G}},t}{\text{maximize}} \quad & t \\
\text{subject to} \quad & \text{SINR}_k \ge t, \\
& \text{SINR}_{e,k} \le \lambda_k, \\
& \sum_{i=1}^{K}\|[\mathbf{W}_k]_n\|_1 + \left\|\widetilde{\mathbf{G}}_n\right\|_1 \le \Delta_n.
\end{aligned} \tag{27}
$$

Next, let us define $\mathbf{W}=\begin{bmatrix}\mathbf{W}_1 & \mathbf{W}_2 & \dots & \mathbf{W}_K\end{bmatrix}$, $\mathbf{Q}=\begin{bmatrix}\mathbf{W} & \widetilde{\mathbf{G}}\end{bmatrix}\in\mathbb{R}^{N_T\times(N_T+K)}$, and $\mathbf{q}=\text{vec}\left(\mathbf{Q}^T\right)$. With the same manner, for a fixed value of t, we solve the feasibility of the following problem

$$
\begin{aligned}
\mathcal{P}6: \ \text{find} \quad & \mathbf{q} \\
\text{subject to} \quad & \|\mathbf{B}_k\mathbf{q}+\boldsymbol{\sigma'}_k\|_F \le \frac{1}{\sqrt{t}}\mathbf{H}_k\left(\mathbf{I}_{N_T}\otimes(\mathbf{e}_k^T\mathbf{V})\right)\mathbf{q}, \\
& \|\mathbf{B}_{e,k}\mathbf{q}+\boldsymbol{\sigma'}_e\|_F \\
& \ge \frac{1}{\sqrt{\lambda_k}}\mathbf{H}_e\left(\mathbf{I}_{N_T}\otimes(\mathbf{e}_k^T\mathbf{V})\right)\mathbf{q}, \\
& -\mathbf{a}\le\mathbf{q}\le\mathbf{a}, \\
& \mathbf{U}\mathbf{a}\le\boldsymbol{\Delta},
\end{aligned} \tag{28}
$$

where $\mathbf{B}_k=\begin{bmatrix}\mathbf{H}_k\otimes\mathbf{I}^k_{N_T+K}\\ \mathbf{0}_{1\times N_T(N_T+K)}\end{bmatrix}$, $\mathbf{B}_{e,k}=\begin{bmatrix}\mathbf{H}_e\otimes\mathbf{I}^k_{N_T+K}\\ \mathbf{0}_{1\times N_T(N_T+K)}\end{bmatrix}$, $\mathbf{V}=\begin{bmatrix}\mathbf{I}_K & \mathbf{0}_{K\times N_T}\end{bmatrix}$, $\mathbf{U}=\mathbf{I}_{N_T}\otimes\mathbf{1}^T_{N_T+K}$, $\boldsymbol{\Delta}=\begin{bmatrix}\Delta_1 & \Delta_2 & \dots & \Delta_{N_T}\end{bmatrix}^T$, $\boldsymbol{\sigma'}_k=\begin{bmatrix}\mathbf{0}_{1\times(N_T+K)} & \sigma'_k\end{bmatrix}^T$, $\boldsymbol{\sigma'}_e=\begin{bmatrix}\mathbf{0}_{1\times(N_T+K)} & \sigma'_e\end{bmatrix}^T$, and $\mathbf{a}=\begin{bmatrix}a_1 & a_2 & \dots & a_{N_T(N_T+K)}\end{bmatrix}^T$ is a new optimization variable. Unlike $\mathcal{P}3$, the above problem is not convex due to the nonconvexity of the constraint on the eavesdropper's SINR. To overcome this issue, we utilize the convex-concave procedure (CCCP) to find a local optimal solution [30], [31]. The CCCP involves an iterative process where at the $i-$th iteration of the procedure, we approximately linearize the convex term $\|\mathbf{B}_{e,k}\mathbf{q}+\boldsymbol{\sigma'}_e\|_F$ using its Taylor expansion as $\left\|\mathbf{B}_{e,k}\mathbf{q}^{(i)}+\boldsymbol{\sigma'}_e\right\|_F \approx \left\|\mathbf{B}_{e,k}\mathbf{q}^{(i-1)}+\boldsymbol{\sigma'}_e\right\|_F + \frac{\left[\mathbf{B}_{e,k}\mathbf{q}^{(i-1)}+\boldsymbol{\sigma'}_e\right]^T\mathbf{B}_{e,k}}{\left\|\mathbf{B}_{e,k}\mathbf{q}^{(i-1)}+\boldsymbol{\sigma'}_e\right\|_F}\left(\mathbf{q}^{(i)}-\mathbf{q}^{(i-1)}\right)$, where $\mathbf{q}^{(i-1)}$ is the value of $\mathbf{q}$ obtained from the previous iteration. As a result, at each iteration of the procedure, problem $\mathcal{P}6$ is approximated to a convex optimization problem $\mathcal{P}7$, which is on the top of this page. The detailed iterative algorithm for solving $\mathcal{P}6$ is summarized as follows

Algorithm 2 Iterative algorithm for solving problem $\mathcal{P}6$

1: **Initialization**
1) Estimate channel matrices $\mathbf{H}_k$, $\mathbf{H}_e$ and noise variances σ_k^2, σ_e^2.
2) Initialize $\mathbf{q}^{(0)}$ to be sufficiently small.

2: **Iteration**: At the $i-$th iteration
1) Update $\mathbf{q}^{(i)}$ given $\mathbf{q}^{(i-1)}$ from previous iteration by solving problem $\mathcal{P}7$ using CVX toolbox .
2) $i=i+1$.

3: **Termination**: terminate the iteration when
1) $\left\|\mathbf{q}^{(i)}-\mathbf{q}^{(i-1)}\right\|\le\epsilon$, where $\epsilon=10^{-3}$ is the predefined threshold, or
2) $i=L$, where $L=10$ is the predefined maximum number of iterations.

IV. AN-AIDED PRECODING DESIGNS USING ZF

In this section, specific designs for the proposed AN-aided precoding scheme using ZF technique are described. ZF aims at decoupling the multi-user channel into multiple independent subchannels, thus simplifies the AN design. Specifically, ZF precoding constructs the precoder $\mathbf{W}_i$ of the $i-$th user in such a way that it is orthogonal to channel matrices of other users, i.e.,

$$
\mathbf{H}_k\mathbf{W}_i=0 \ \ \forall k\ne i. \tag{29}
$$

For mathematical connivence, we can express the above equations in a more compact form as follows

$$
\mathbf{H}\mathbf{W}=\begin{bmatrix}\sqrt{q_1} & & & \\ & \sqrt{q_2} & & \\ & & \ddots & \\ & & & \sqrt{q_K}\end{bmatrix}=\text{diag}\{\sqrt{\mathbf{q}}\}, \tag{30}
$$

where $\sqrt{\mathbf{q}}=\begin{bmatrix}\sqrt{q_1} & \sqrt{q_2} & \dots & \sqrt{q_K}\end{bmatrix}^T\in\mathbb{R}^{1\times K}$ whose $i-$th element represents the $i-$th user's channel gain. $\mathbf{W}$ can then be written in the following form

$$
\mathbf{W}=\mathbf{H}^{-}\text{diag}\{\sqrt{\mathbf{q}}\}, \tag{31}
$$

where $\mathbf{H}^{-}$ is the generalized inverse of $\mathbf{H}$, which can be any matrix that satisfies $\mathbf{H}\mathbf{H}^{-}\mathbf{H}=\mathbf{H}$. Generally, with the

assumption that $\mathbf{H}$ is full row-rank, any generalized inverses $\mathbf{H}^-$ can be expressed by

$$\mathbf{H}^- = \mathbf{H}^\dagger + \mathbf{PQ}, \tag{32}$$

where $\mathbf{H}^\dagger = \mathbf{H}^T(\mathbf{H}\mathbf{H}^T)^{-1}$ is the pseudo-inverse of $\mathbf{H}$, $\mathbf{P} = \mathbf{I} - \mathbf{H}^\dagger\mathbf{H}$ is the projection onto the null space of $\mathbf{H}$ and $\mathbf{Q}$ is an arbitrary matrix. Then, the general structure of any ZF precoding matrix $\mathbf{W}$ is given by

$$\mathbf{W} = \left[\mathbf{H}^\dagger + \mathbf{PQ}\right] \text{diag}\{\sqrt{\mathbf{q}}\}. \tag{33}$$

With this expression, the AN design problems reduce to optimization problems with respect to $\mathbf{q}$ and the choice of $\mathbf{Q}$.

A. UNKNOWN EAVESDROPPER'S CSI

With ZF precoding, the SINR of the $k-$th user is given by

$$\text{SINR}_k^{\text{ZF}} = \frac{|\mathbf{H}_k\mathbf{W}_k|^2}{\sigma_k'^2} = \frac{q_k}{\sigma_k'^2}, \tag{34}$$

The max-min fairness problem is formulated as

$$\begin{aligned} \mathcal{P}8: \underset{\mathbf{W}_k}{\text{maximize}} \quad & \min_k \ \frac{q_k}{\sigma_k'^2} \\ \text{subject to} \quad & \mathbf{HW} = \text{diag}\{\sqrt{\mathbf{q}}\}, \\ & \sum_{i=1}^{K} \|[\mathbf{W}_k]_n\|_1 + \rho_n \|\mathbf{G}_n\|_1 \le \Delta_n. \end{aligned} \tag{35}$$

Similar to the case of general design, we assume that ρ_n's are set equally at all LED transmitters. Let us define $\boldsymbol{\sigma}'^2 = \begin{bmatrix}\sigma_1'^2 & \sigma_2'^2 & \dots & \sigma_K'^2\end{bmatrix}^T$ and $\text{diag}\{\mathbf{q}'\} = \text{diag}\{\mathbf{q}\}\text{diag}\{\boldsymbol{\sigma}'^2\}$ where $\mathbf{q}' = \begin{bmatrix}q_1' & q_2' & \dots & q_K'\end{bmatrix}$. Then, $\mathcal{P}8$ can be rewritten as

$$\begin{aligned} \mathcal{P}9: \quad \underset{\mathbf{W}_k}{\text{maximize}} \quad & \min_k \ q_k' \\ \text{subject to} \quad & \mathbf{HW} = \text{diag}\{\sqrt{\mathbf{q}'}\}\text{diag}\{\boldsymbol{\sigma}'\}, \\ & \|[\mathbf{W}]_n\|_1 \le \Delta_{\overline{\rho},n}. \end{aligned} \tag{36}$$

In the above problem, the optical power constraint has been rewritten with respect to $\mathbf{W}$. Following the similar argument in [33], we can search the optimal solution of the form $\mathbf{q}' = q'\mathbf{1}$ for some q' is optimal. To see this, let $\mathbf{W}^*$ and $\mathbf{q}^*$ be the optimal solution to $\mathcal{P}9$ and we define new variables $\mathbf{q}' = \overline{q}\mathbf{1}$ and $\mathbf{W} = \mathbf{W}^*\text{diag}\left\{\begin{bmatrix}\sqrt{\overline{q}/q_1^*} & \dots & \sqrt{\overline{q}/q_K^*}\end{bmatrix}\right\}$, where $\overline{q} = \min_k q_k^*$. Then, it holds that

$$\begin{aligned} \mathbf{HW} &= \mathbf{HW}^*\text{diag}\left\{\begin{bmatrix}\sqrt{\overline{q}/q_1^*} & \dots & \sqrt{\overline{q}/q_K^*}\end{bmatrix}\right\} \\ &= \text{diag}\{\sqrt{\mathbf{q}^*}\}\text{diag}\{\sqrt{\boldsymbol{\sigma}}\}\text{diag}\left\{\begin{bmatrix}\sqrt{\overline{q}/q_1^*} & \dots & \sqrt{\overline{q}/q_K^*}\end{bmatrix}\right\} \\ &= \text{diag}\{\sqrt{\mathbf{q}'}\}\text{diag}\{\sqrt{\boldsymbol{\sigma}}\}, \end{aligned} \tag{37}$$

and

$$\begin{aligned} \|[\mathbf{W}]_n\|_1 &= \left\|\left[\mathbf{W}^*\text{diag}\left\{\begin{bmatrix}\sqrt{\overline{q}/q_1^*} & \dots & \sqrt{\overline{q}/q_K^*}\end{bmatrix}\right\}\right]_n\right\|_1 \\ &\le \|[\mathbf{W}^*]_n\|_1, \end{aligned} \tag{38}$$

since $\overline{q}/q_k^* \le 1$ for all k. That is, $\mathbf{W}$ and $\mathbf{q}'$ are also feasible and offer the same objective. We thus can reduce $\mathcal{P}9$ to

$$\begin{aligned} \mathcal{P}10: \quad \underset{q'\ge 0,\mathbf{Q}}{\text{maximize}} \quad & q' \\ \text{subject to} \quad & \sqrt{q'\sigma_n^2}\left\|\left[\mathbf{H}^\dagger + \mathbf{PQ}\right]_n\right\|_1 \le \Delta_{\overline{\rho},n}. \end{aligned}$$

It is easy to see that the optimal solution q'_{opt} is given by

$$q'_{\text{opt}} = \min_n \frac{\Delta_{\overline{\rho},n}^2}{\sigma_n' \left\|\left[\mathbf{H}^\dagger + \mathbf{PQ}\right]_n\right\|_1^2}, \tag{39}$$

where $\mathbf{Q}$ is the solution to

$$\begin{aligned} \mathcal{P}11: \quad \underset{\mathbf{Q},t}{\text{minimize}} \quad & t \\ \text{subject to} \quad & \sigma_n' \left\|\left[\mathbf{H}^\dagger + \mathbf{PQ}\right]_n\right\|_1^2 \le t. \end{aligned}$$

It can be seen that the above problem is a linear programming, which has been well studied in literature and can be solved efficiently using off-the-self optimization packages.

B. KNOWN EAVESDROPPER'S CSI

In this case, the SINR of the $k-$ user is simplified as

$$\text{SINR}_k^{\text{ZF}} = \frac{|\mathbf{H}_k\mathbf{W}_k|^2}{\left\|\mathbf{H}_k\widetilde{\mathbf{G}}\right\|_F^2 + \sigma_k'^2}. \tag{40}$$

Since ZF is only applied to legitimate users, the expression for the SINR of the eavesdropper is the same to that in (25). The max-min fairness problem is then given by

$$\begin{aligned} \mathcal{P}12: \underset{\mathbf{W}_k,\widetilde{\mathbf{G}}}{\text{maximize}} \quad & \min_k \ \text{SINR}_k^{\text{ZF}} \\ \text{subject to} \quad & \text{SINR}_{e,k}^{\text{ZF}} \le \lambda_k, \\ & \mathbf{H}_i\mathbf{W}_k = 0 \ \ \forall k \ne i, \\ & \sum_{i=1}^{K} \|[\mathbf{W}_k]_n\|_1 + \left\|\widetilde{\mathbf{G}}_n\right\|_1 \le \Delta_n, \end{aligned} \tag{41}$$

It can be seen that it is difficult to handle the above problem by using of the expression in (33) due to the involvement of $\mathbf{G}$ in both objective function and constraints. Instead, we follow the same procedure as in the case of the general design described in Section III. B to reformulate $\mathcal{P}11$ to a convex optimization problem. With the same variable transformations as in $\mathcal{P}6$, we solve the feasibility of the following problem

$$\begin{aligned} \mathcal{P}13: \text{find} \quad & \mathbf{q} \\ \text{subject to} \quad & \|\mathbf{B}_k\mathbf{q} + \boldsymbol{\sigma}'_k\|_F \le \frac{1}{\sqrt{t}}\mathbf{H}_k\left(\mathbf{I}_{N_T} \otimes (\mathbf{e}_k^T\mathbf{V})\right)\mathbf{q}, \\ & \|\mathbf{B}_{e,k}\mathbf{q} + \boldsymbol{\sigma}'_e\|_F \\ & \ge \frac{1}{\sqrt{\lambda_k}}\mathbf{H}_e\left(\mathbf{I}_{N_T} \otimes (\mathbf{e}_k^T\mathbf{V})\right)\mathbf{q}, \\ & \mathbf{H}_k\left(\mathbf{I}_{N_T} \otimes (\mathbf{e}_i^T\mathbf{V})\right)\mathbf{q} = 0, \ \forall k \ne i, \\ & -\mathbf{a} \le \mathbf{q} \le \mathbf{a}, \\ & \mathbf{U}\mathbf{a} \le \boldsymbol{\Delta}. \end{aligned} \tag{42}$$

Similar to $\mathcal{P}6$, the CCCP can be used to solve the above problem.

Table 1: System Parameters

Room and LED configurations	
Room dimension (Length × Width × Height)	5 (m) × 5 (m) × 3 (m)
LED array positions	array 1 : $(-\sqrt{2}, -\sqrt{2}, 3)$ array 2 : $(\sqrt{2}, -\sqrt{2}, 3)$ array 3 : $(\sqrt{2}, \sqrt{2}, 3)$ array 4 : $(-\sqrt{2}, \sqrt{2}, 3)$
LED bandwidth, B	20 MHz
LED beam angle, ϕ (LED Lambertian order is 1)	120°
LED conversion factor, η	0.44 W/A
Receiver photodetectors	
PD active area, A_r	1 cm^2
PD responsivity, γ	0.54 A/W
PD field of view (FOV), Ψ	60°
Optical filter gain, $T_s(\psi)$	1
Refractive index of the concentrator, κ	1.5
Other parameters	
Ambient light photocurrent, χ_{amp}	10.93 A/(m^2 · Sr)
Preamplifier noise current density, i_{amp}	5 pA/Hz$^{-1/2}$

V. NUMERICAL RESULTS AND DISCUSSIONS

In this section, numerical results are presented to demonstrate the performances of the two AN-aided precoding designs presented in previous sections. The geographical configuration of the considered system, which consists of 4 LED arrays, is shown in Fig. 1. We assume that legitimate users and the eavesdropper are located on a receive plane, which is 0.5 m above the floor. For the position specification, a Cartesian coordinate system whose the origin is the center of the floor is used. In addition, all simulation results are obtained by averaging $5,000$ different channel realizations (i.e., $5,000$ different positions of legitimate users and eavesdropper uniformly placed on the receive plane). For the sake of conciseness, simulation results are illustrated for the case of 2 legitimate users. Furthermore, assume that the DC-bias I_n^{DC} are the same for all LED arrays (i.e., $I_i^{\text{DC}} = I^{\text{DC}_j} = I_0^{\text{DC}}$). Unless otherwise noted, the parameters of the room, LED arrays and optical receivers are given in Table 1.

For the case of unknown eavesdropper's CSI, Fig. 3 presents the SINR performances of legitimate users and the eavesdropper with respect to the AN power adjusting factor $\overline{\rho}$. The average LED array power $P_0 = \mu I_0^{\text{DC}}$ is set to 35 dBm. As we showed in Section IV.A that the ZF design has the optimal solution where users' SINR are equal. It also holds in the case of general design as numerically illustrated in the figure. We also observed that significant gaps between users' and eavesdropper's SINRs are achieved in both designs, thus ensuring high secrecy capacity performances. For example at $\rho = 0.9$, the performance gaps are 40 dB and 36 dB in case of general and ZF designs, respectively.

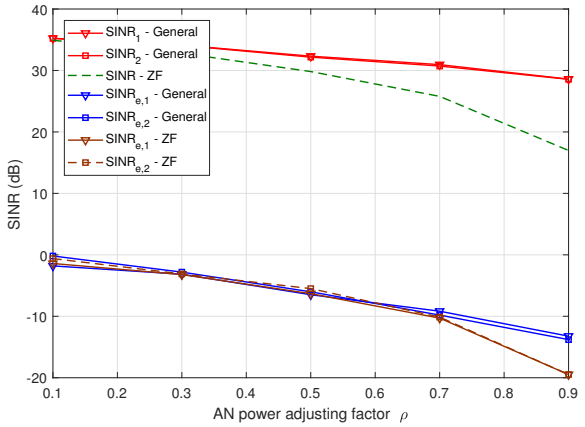

Figure 3: SINR performances of legitimate users and the eavesdropper versus $\overline{\rho}$: unknown eavesdropper's CSI.

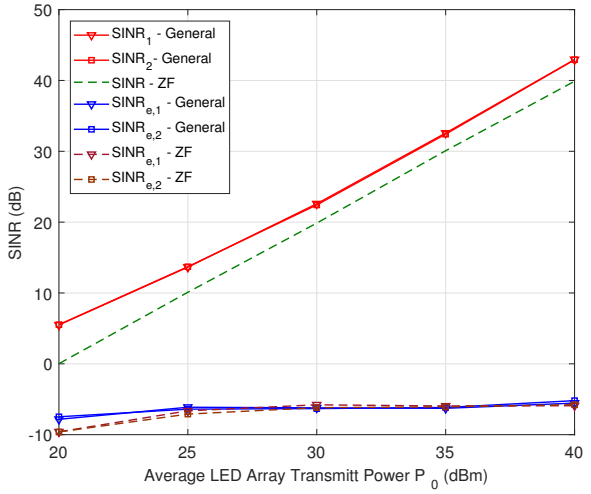

Figure 4: SINR performances of legitimate users and the eavesdropper versus average LED array power: known eavesdropper's CSI.

In Fig. 4, the fairness performances versus average LED transmit power are illustrated. The AN power adjusting factor $\rho = 0.5$ is set. It is seen that the general design, which optimizes users' SIRNs output, outperforms the ZF one, especially at lower transmit power. At high transmit power regimes, the performance of the ZF design approaches that of the general one. This reflects the fact that ZF precoding achieves good performance at high transmit power [33]. It is also seen that the eavesdropper's SINRs in case of ZF design are lower than those of the general one at the low transmit power region. However, they are almost the same when the LED transmit power increases.

For the case of known $\mathbf{H}_e$, Fig. 5 depicts the max-min fairness performances in accordance to the average LED transmit power for different values of eavesdropper's SINR

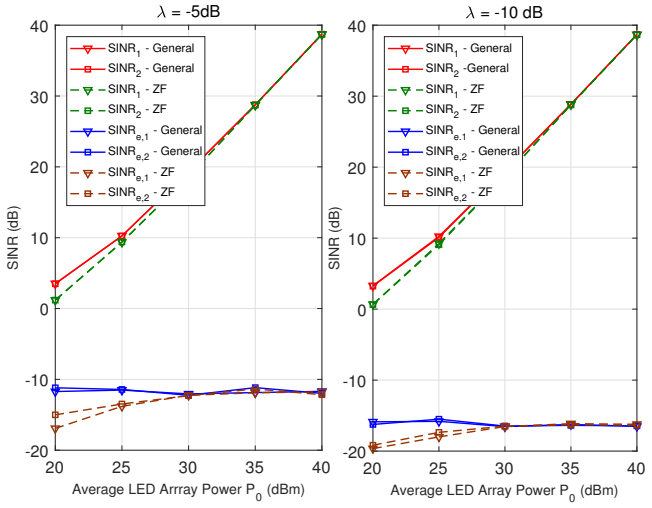

Figure 5: SINR performances of legitimate users and the eavesdropper versus average LED array power: known eavesdropper's CSI.

threshold, $\lambda = -5$ and -10 dB. Similar to the case of unknown $\mathbf{H}_e$, we also observed significant gaps between users' and eavesdropper' SINR in both general and ZF designs. Interestingly, while the eavesdropper's SINRs are kept almost constant in case of general design, they increase according to an increase in the transmit power in case of ZF design.

VI. CONCLUSIONS

The paper studied AN-aided precoding designs for multi-user MISO-VLC broadcast systems with the presence of an eavesdropper. In case the eavesdropper's CSI is not available, the AN was designed to lie on the null-space of the users' channel. When the eavesdropper's CSI is available, the design aimed at limiting the eavesdropper's SINR below a certain threshold. A specific AN design, which utilizes ZF was also examined. In case of unknown eavesdropper's CSI, numerical results showed that, for the both designs (i.e., general and ZF), significant gaps between users' and eavesdropper's SINR were achieved. In case of known eavesdropper's CSI and general design, it was observed that, the eavesdropper' SINRs were kept almost constant regardless of the transmitted power. In case of ZF design, the eavesdropper's SINR increased in accordance to an increase of the transmitted power. Similar to the case of unknown eavesdropper's CSI, both designs provided a sufficient secrecy level.

References

[1] P. H. Pathak, X. Feng, P. Hu, and P. Mohapatra, "Visible light communication, networking, and sensing: a survey, potential and challenges," *IEEE Commun. Surveys Tuts.*, vol. 17, no. 4, pp. 2047–2077, Sept. 2015.

[2] A. Jovicic, L. Junyi, T. Richardson, "Visible light communication: opportunities, challenges and the path to market," *IEEE Commun. Mag.*, vol. 51, no. 12, pp. 26–32, Dec. 2013.

[3] L. Zeng, D. O'Brien, H. Minh, G. Faulkner, K. Lee, D. Jung, Y. J. Oh, E.T. Won, "High data rate multiple input multiple output (MIMO) optical wireless communications using white led lighting," *IEEE J. Sel. Areas Commun.*, vol. 27, no. 9, pp. 1654–1662, 2009.

[4] T. Fath, H. Haas, "Performance comparison of MIMO techniques for optical wireless communications in indoor environments," *IEEE Trans. Commun.*, vol. 61, no. 2, pp. 733–742, Feb. 2013.

[5] L. Wu, Z. Zhang and H. Liu, "MIMO-OFDM visible light communications system with low complexity," in *Proc. IEEE International Conference Communications (ICC)*, pp. 3933–3937, June 2013.

[6] A. Burton, *et al.*, "Experimental demonstration of 50-Mb/s visible light communications using 4 × 4 MIMO," *IEEE Photon. Technol. Lett.*, vol. 26, no. 9, pp. 945–948, May 2014.

[7] A. Nuwanpriya, S. W. Ho, C. S. Chen, "Indoor MIMO visible light communications: novel angle diversity receivers for mobile users," *IEEE J. Sel. Areas Commun.*, vol. 33, no. 9, pp. 1780–1792, Sept. 2015.

[8] H. Ma, L. Lampe, S. Hranilovic, "Coordinated broadcasting for multiuser indoor visible light communication systems," *IEEE Trans. Commun.*, vol. 63, no. 9, pp. 3313–3324, Sept. 2015.

[9] B. Li, J. Wang, R. Zhang, H. Shen, C. Zhao, L. Hanzo, "Multiuser MISO transceiver design for indoor downlink visible light communication under per-LED optical power constraints," *IEEE Photon. J.*, vol. 7, no. 4, Aug. 2015, Art. ID 7201415.

[10] T. V. Pham, H. Le-Minh, A. T. Pham, "Multi-user visible light communication broadcast channels with zero-forcing precoding," *IEEE Trans. Commun.*, vol. 64, no. 6, pp. 2509–2521, June 2017.

[11] A. D. Wyner, "The wire-tap channel," *Bell Syst. Tech. J.*, vol. 54, pp. 1355–1387, 1975.

[12] I. Csiszar, J. Korner, "Broadcast channels with confidential messages," *IEEE Trans. Info. Theory*, vol. 24, no. 3, pp. 339–348, May 1978.

[13] S. L. Y. Cheong, M. Hellman, "The Gaussian wire-tap channel," *IEEE Trans. Info. Theory*, vol. 24, no. 4, pp. 451–456, July 1978.

[14] A. Mostafa, L. Lampe, "Physical-layer security for MISO visible light communication channels," *IEEE J. Sel. Areas Commun.*, vol. 33, no. 9, pp. 1806–1811, Sept. 2015.

[15] S. Ma, Z-L. Dong, H. Li, Z. Lu, S. Li, "Optimal and robust secure beamformer for indoor MISO visible light communication," *J. Lightwave Technol.*, vol. 34, no. 21, pp. 4988–4998, Nov. 2016.

[16] A. Mostafa, L. Lampe, "Optimal and robust beamforming for secure transmission in MISO visible light communication links," *IEEE Trans. Signal Process.*, vol. 64, no. 24, pp. 6501–6516, Dec. 2016.

[17] T. V. Pham, A. T. Pham, "Secrecy sum-rate of multi-user MISO visible light communication systems with confidential messages," *Elsevier Optik,* vol. 151, pp. 65–76, Dec. 2017.

[18] S. Cho, G. Chen, J. P. Coon, "Securing visible light communication systems by beamforming in the presence of randomly distributed eavesdroppers," *IEEE Trans. Wireless Commun.*, vol. 17, no. 5, pp. 2918–2931, Feb. 2018.

[19] X. Zhao, H. Chen, J. Sun, "On physical-layer security in multiuser visible light communication systems with non-orthogonal multiple access," *IEEE Access*, vol. 6, pp. 34004–34017, June 2018.

[20] J-Y. Wang, C. Liu, J-B. Wang, Y. Wu, M. Lin, J. Cheng, "Physical-layer security for indoor visible light communications: secrecy capacity analysis," *IEEE Trans. Commun.*, DOI: 10.1109/TCOMM.2018.2859943, July 2018.

[21] A. Mostafa, L. Lampe, "Securing visible light communications via friendly jamming," in *Proc. IEEE Global Communications Conference (GLOBECOM), Workshop on Optical Wireless Communications*, Dec. 2014.

[22] H. Zaid, Z. Rezki, A. Chaaban, M. S. Alouini, "Improved achievable secrecy rate of visible light communication with cooperative jamming," in *Proc. Symposium of Signal Processing for Optical Wireless Communications*, pp. 1165–1169, Dec. 2015.

[23] H. Shen, Y. Deng, W. Xu, C. Zhao, "Secrecy-oriented transmitter optimization for visible light communication systems," *IEEE Photon J.*, vol. 8, no. 5, Oct. 2016, Art. ID 7905914.

[24] H. Arfaoui, Z. Rezki, A. Ghrayeb, M. S. Alouini, "On the secrecy capacity of MISO visible light communication channels," in *Proc. IEEE Global Communications Conference (GLOBECOM)*, Dec. 2016.

[25] T. V. Pham, T. Hayashi, A. T. Pham, "Artificial-noise-aided precoding design for multi-user visible light communication channels," in *Proc. IEEE International Conference on Communications (ICC), Workshop on Optical Wireless Communications*, May 2018.

[26] J. G. Smith, "The information capacity of amplitude and variance-constrained scalar Gaussian channels," *J. Inf. Control*, vol. 18, no. 3, pp. 203–219, Apr. 1971.

[27] T. Komine, M. Nakagawa, "Fundamental analysis for visible-light communication system using LED lights," *IEEE Trans. Consum. Electron.*, vol. 50, no. 1, pp. 100–107, Feb. 2004.

[28] T. Cover, J. Thomas, "Elements of information theory," *Wiley Interscience*, 2006.
[29] H. Sifaou, K. H. Park, A. Kammoun, M. S. Alouini, "Optimal linear precoding for indoor visible light communication system," in *Proc. IEEE International Conference on Communications (ICC)*, May 2017.
[30] A. L. Yuille, A. Rangarajan, "The concave-convex procedure (CCCP)," *Neural Comput.*, vol. 15, no. 4, pp. 915–936, 2003.
[31] B. K. Sriperumbudur, G. R. G. Lanckriet, "On the convergence of the concave-convex procedure," in *Proc. Neural Inf. Process. Syst.*, pp. 1–9, 2009.
[32] M. S. Lobo, L. Vandenberghe, S. Boyd, H. Lebret, "Applications of second-order cone programming," *Linear Algebra Appl.*, vol. 284, no. 1-3, pp. 193–228, Nov. 1998.
[33] A. Wiesel, Y. C. Eldar, S. Shamai, "Zero-forcing precoding and generalized inverses," *IEEE Trans. Signal Process.*, vol. 56, no. 9, pp. 4409–4418, Sept. 2008.
[34] M. Grant, S. Boyd, "CVX: Matlab software for disciplined convex programming version 2.1," *http://cvxr.com/cvx/*, Jan. 2015.
[35] J. Lofberg, "YALMIP: a toolbox for modeling and optimization in MATLAB," in *Proc. IEEE Int. Symp. on Computer Aided Control Systems Design*, pp. 284–289, Sept. 2004.